J|A|C|S
ARTICLES
Published on Web 03/29/2006

Molecular Self-Assembly at Bare Semiconductor Surfaces: Preparation and Characterization of Highly Organized Octadecanethiolate Monolayers on GaAs(001)

Christine L. McGuiness,[†] Andrey Shaporenko,[‡] Carole K. Mars,[†,§] Sundararajan Uppili,[†] Michael Zharnikov,[‡] and David L. Allara*[,†]

Contributions from the Departments of Chemistry and Materials Science, The Pennsylvania State University, 104 Chemistry Building, University Park, Pennsylvania 16801-6300, and Angewandte Physikalische Chemie, Universität Heidelberg, Im Neuenheimer Feld 253, D-69120 Heildelberg, Germany

Received December 21, 2005; E-mail: dla3@psu.edu

Abstract: Through rigorous control of preparation conditions, organized monolayers with a highly reproducible structure can be formed by solution self-assembly of octadecanethiol on GaAs (001) at ambient temperature. A combination of characterization probes reveal a structure with conformationally ordered alkyl chains tilted on average at $14 \pm 1°$ from the surface normal with a $43 \pm 5°$ twist, a highly oleophobic and hydrophobic ambient surface, and direct S−GaAs attachment. Analysis of the tilt angle and film thickness data shows a significant mismatch of the average adsorbate molecule spacings with the spacings of an intrinsic GaAs(001) surface lattice. The monolayers are stable up to ~100 °C and exhibit an overall thermal stability which is lower than that of the same monolayers on Au{111} surfaces. A two-step solution assembly process is observed: rapid adsorption of molecules over the first several hours to form disordered structures with molecules lying close to the substrate surface, followed by a slow densification and asymptotic approach to final ordering. This process, while similar to the assembly of alkanethiols on Au{111}, is nearly 2 orders of magnitude slower. Finally, despite differences in assembly rates and the thermal stability, exchange experiments with isotopically tagged molecules show that the octadecanethiol on GaAs(001) monolayers undergo exchange with solute thiol molecules at roughly the same rate as the corresponding exchanges of the same monolayers on Au{111}.

1. Introduction

The ability to modify and control the surface properties of a variety of materials by the formation of dense, conformal self-assembled monolayer (SAM) coatings has become a significant scientific and technological tool in recent years.[1−5] The major focus has been on divalent organosulfur molecules, particularly thiols chemisorbed on noble metals, and on various Lewis and Brönsted acids or bases chemisorbed on inorganic oxide surfaces. Despite the enormous technological importance of semiconductor materials there are relatively few studies of surface self-assembly involving direct attachment to the semiconductor, primarily because of the challenging surface chemistry. In particular, the strong propensity to form oxides becomes problematic given the typical wet chemical conditions needed for the chemisorption of moderately sized molecules with varied functionality. The majority of literature reports for such solution assembly have involved the technologically important group IV and III−V semiconductors. In the case of the former, attachment of molecular films directly to Si and Ge surfaces through Si−O−Si,[1,6,7,] Si−C,[8−10] Ge−C,[10,11] and Ge−S covalent bonding[12,13] has been reported, but almost all cases, except perhaps Ge−S, involve high energy bonds which prevent self-organization of the grafted molecules.

In the case of III−V materials, a number of reports of molecular monolayers have appeared, but most involve film formation on the oxide covered substrate.[14−18] Direct bonding

[†] The Pennsylvania State University.
[‡] Universität Heidelberg.
[§] Present address: Novellus Systems, 11155 SW Leveton Drive, Tualatin, Oregon 97062.

(1) Ulman, A. *Chem. Rev.* **1996**, *96*, 1533−1554.
(2) Love, J. C.; Estroff, L. A.; Kriebel, J. K.; Nuzzo, R. G.; Whitesides, G. M. *Chem. Rev.* **2005**, *105*, 1103−1169.
(3) Smith, R. K.; Lewis, P. A.; Weiss, P. S. *Prog. Surf. Sci.* **2004**, *75*, 1−68.
(4) Joachim, C.; Gimzewski, J. K.; Aviram, A. *Nature* **2000**, *408*, 541−548.
(5) Gates, B. D.; Xu, Q. B.; Stewart, M.; Ryan, D.; Willson, C. G.; Whitesides, G. M. *Chem. Rev.* **2005**, *105*, 1171−1196.
(6) Maoz, R.; Sagiv, J. J. *Colloid Interface Sci.* **1984**, *100*, 465−496.
(7) Bigelow, W. C.; Pickett, D. L.; Zisman, W. A. *J. Colloid. Sci.* **1946**, *101*, 201.
(8) Stewart, M. P.; Maya, F.; Kosynkin, D. V.; Dirk, S. M.; Stapleton, J. J.; McGuiness, C. L.; Allara, D. L.; Tour, J. M. *J. Am. Chem. Soc.* **2004**, *126*, 370−378.
(9) Linford, M. R.; Chidsey, C. E. D. *J. Am. Chem. Soc.* **1993**, *115*, 12631−12632.
(10) Buriak, J. M. *Chem. Rev.* **2002**, *102*, 1271−1308.
(11) He, J. L.; Lu, Z. H.; Mitchell, S. A.; Wayner, D. D. M. *J. Am. Chem. Soc.* **1998**, *120*, 2660−2661.
(12) Kosuri, M. R.; Cone, R.; Li, Q. M.; Han, S. M.; Bunker, B. C.; Mayer, T. M. *Langmuir* **2004**, *20*, 835−840.
(13) Han, S. M.; Ashurst, W. R.; Carraro, C.; Maboudian, R. *J. Am. Chem. Soc.* **2001**, *123*, 2422−2425.
(14) Hasegawa, T.; Nishijo, J.; Umemura, J.; Theiss, W. *J. Phys. Chem. B* **2001**, *105*, 11178−11185.
(15) Bastide, S.; Butruille, R.; Cahen, D.; Dutta, A.; Libman, J.; Shanzer, A.; Sun, L. M.; Vilan, A. *J. Phys. Chem. B* **1997**, *101*, 2678−2684.

to GaAs surfaces appears to occur under a variety of reaction conditions for small halogenated alkane molecules,[19−21] aryl diazonium salts,[8] and small chalcogenide molecules.[19] Monolayer films of organic thiols have also been shown to form on GaAs,[22−42] InP,[27,43−45] and InAs.[46] Despite this extensive body of research no definitive demonstration has been made to our knowledge of the formation of crystalline ordered, self-organized monolayers with direct bonding to any of these bare substrates. Clearly, it would be a significant advance to develop classes of highly dense, ordered SAMs for these materials, similar to the types now well-known for the alkanethiolate/Au{111} system.[2]

Driven in good part by our interest in hybrid molecule-semiconductor devices, we have continued to explore the development of simple methods to form translationally ordered SAMs on bare semiconductors with direct molecule−substrate bonding. The formation of long alkyl chain types of SAMs are particularly useful systems on which to focus given the extensive knowledge and literature on the analogous SAMs on Au{111}[1−3] and the well-known driving force of the long alkyl chains to order. Inspired by well-known inorganic sulfide passivation treatments which had shown that the native oxide of GaAs could be extensively removed to give direct bonding of S species to the GaAs surface with dramatic improvement in the important electronic properties of the semiconductor,[47−50] we showed in an early report that octadecanethiol (**ODT)** -based SAMs could be formed on GaAs(001) by exposure of the cleaned substrate to pure, molten thiol at elevated temperatures.[22,23] These SAMs exhibited dominantly all-*trans* alkyl chains with an average 57° tilt angle of the long molecular axis from the surface normal, a thickness of ∼14 Å, and static water and hexadecane contact angles of 103−109° and 41 ± 2°, respectively.[23,51] The striking contrast with the molecular orientation and film thickness of ∼28° and ∼23 Å, respectively, for **ODT** SAMs on Au{111} surfaces[1,23,52,53] indicated significantly different structures for the two classes of monolayers. Subsequent studies showed that simpler preparation conditions using ethanolic solutions of **ODT** were possible,[40−42] with later variations including specific oxide etchants[37,39] to minimize oxide formation. The net outcome of all this work has been a significant controversy concerning critical characteristics of **ODT**/GaAs(001) SAMs, both for the same preparation method and between different types of preparations. For example, with regard to structural features, characterizations of the SAMs formed from ethanolic solutions have shown a range of thicknesses from 12 to 20 Å as measured by a variety of techniques including single wavelength ellipsometry (SWE),[37,54] capacitance measurements,[37,38] and X-ray photoelectron spectroscopy (XPS).[39] Further, one atomic force microscopy (AFM) study[36] has reported that assembly in ethanolic solution leads to smoother surfaces than those for molten thiol. In addition, based on high-resolution images of the different treatments it was suggested that both preparation conditions lead to a different adlayer lattice than the intrinsic square lattice structure of GaAs obtained with inorganic sulfide treatments. The nature of the thiol−GaAs interface also has been the subject of controversy with reports of Ga−S bonding,[32,34] As−S bonding,[26,35,37,39,55] and even direct thiol attachment with no observation of either Ga−S or As−S bonding.[28,29,33] Finally, while one of the advantages of these SAMs is their stability against oxidation of the GaAs substrate, little quantitative information is available. It has been reported that in cases of oxygen-free storage the monolayers are stable and resist monolayer degradation for at least 4 months,[30] but other stability experiments indicate these monolayers are stable for a lesser amount of time.[38,56−58]

In retrospect, it is not surprising that there are many inconsistencies in the characteristics of the SAMs from prepara-

(16) do Rego, A. M. B.; Ferraria, A. M.; El Beghdadi, J.; Debontridder, F.; Brogueira, P.; Naaman, R.; Vilar, M. R. *Langmuir* **2005**, *21*, 8765−8773.
(17) Ashkenasy, G.; Cahen, D.; Cohen, R.; Shanzer, A.; Vilan, A. *Acc. Chem. Res.* **2002**, *35*, 121−128.
(18) Vilan, A.; Ussyshkin, R.; Gartsman, K.; Cahen, D.; Naaman, R.; Shanzer, A. *J. Phys. Chem. B* **1998**, *102*, 3307−3309.
(19) Seker, F.; Meeker, K.; Kuech, T. F.; Ellis, A. B. *Chem. Rev.* **2000**, *100*, 2505−2536.
(20) Khan, K. A.; Camillone, N.; Osgood, R. M. *J. Phys. Chem. B* **1999**, *103*, 5530−5542.
(21) Khan, K. A.; Camillone, N.; Osgood, R. M. *J. Chem. Phys.* **1999**, *110*, 10526−10538.
(22) Nakagawa, O. S.; Ashok, S.; Sheen, C. W.; Martensson, J.; Allara, D. L. *Jpn. J. Appl. Phys., Part 1* **1991**, *30*, 3759−3762.
(23) Sheen, C. W.; Shi, J. X.; Martensson, J.; Parikh, A. N.; Allara, D. L. *J. Am. Chem. Soc.* **1992**, *114*, 1514−1515.
(24) Hou, T.; Greenlief, M.; Keller, S. W.; Nelen, L.; Kauffman, J. F. *Chem. Mater.* **1997**, *9*, 3181−3186.
(25) Adlkofer, K.; Eck, W.; Grunze, M.; Tanaka, M. *J. Phys. Chem. B* **2003**, *107*, 587−591.
(26) Shaporenko, A.; Adlkofer, K.; Johansson, L. S. O.; Tanaka, M.; Zharnikov, M. *Langmuir* **2003**, *19*, 4992−4998.
(27) Adlkofer, K.; Shaporenko, A.; Zharnikov, M.; Grunze, M.; Ulman, A.; Tanaka, M. *J. Phys. Chem. B* **2003**, *107*, 11737−11741.
(28) Lunt, S. R.; Ryba, G. N.; Santangelo, P. G.; Lewis, N. S. *J. Appl. Phys.* **1991**, *70*, 7449−7465.
(29) Lunt, S. R.; Santangelo, P. G.; Lewis, N. S. *J. Vac. Sci. Technol., B* **1991**, *9*, 2333−2336.
(30) Dorsten, J. F.; Maslar, J. E.; Bohn, P. W. *Appl. Phys. Lett.* **1995**, *66*, 1755−1757.
(31) Lu, E. D.; Zhang, F. P.; Xu, S. H.; Yu, X. J.; Xu, P. S.; Han, Z. F.; Xu, F. Q.; Zhang, X. Y. *Appl. Phys. Lett.* **1996**, *69*, 2282−2284.
(32) Yang, G. H.; Zhang, Y.; Kang, E. T.; Neoh, K. G.; Huang, W.; Teng, J. H. *J. Phys. Chem. B* **2003**, *107*, 8592−8598.
(33) Camillone, N.; Khan, K. A.; Osgood, R. M. *Surf. Sci.* **2000**, *453*, 83−102.
(34) Donev, S.; Brack, N.; Paris, N. J.; Pigram, P. J.; Singh, N. K.; Usher, B. F. *Langmuir* **2005**, *21*, 1866−1874.
(35) Cho, Y.; Ivanisevic, A. *J. Phys. Chem. B* **2005**, *109*, 12731−12737.
(36) Ke, Y.; Milano, S.; Wang, X. W.; Tao, N.; Darici, Y. *Surf. Sci.* **1998**, *415*, 29−36.
(37) Adlkofer, K.; Tanaka, M. *Langmuir* **2001**, *17*, 4267−4273.
(38) Adlkofer, K.; Tanaka, M.; Hillebrandt, H.; Wiegand, G.; Sackmann, E.; Bolom, T.; Deutschmann, R.; Abstreiter, G. *Appl. Phys. Lett.* **2000**, *76*, 3313−3315.
(39) Ye, S.; Li, G. F.; Noda, H.; Uosaki, K.; Osawa, M. *Surf. Sci.* **2003**, *529*, 163−170.
(40) Mars, C. K.; Allara, D. L. *Abstr. Pap. Am. Chem. S.* **1998**, *216*, U629.
(41) Mars, C. K. Growth and Characterization of Self-Assembled Molecular Monolayers on Gallium Arsenide. The Pennsylvania State University, University Park, Pennsylvania, 2000.
(42) Baum, T.; Ye, S.; Uosaki, K. *Langmuir* **1999**, *15*, 8577−8579.
(43) Lim, H.; Carraro, C.; Maboudian, R.; Pruessner, M. W.; Ghodssi, R. *Langmuir* **2004**, *20*, 743−747.
(44) Schvartzman, M.; Sidorov, V.; Ritter, D.; Paz, Y. *J. Vac. Sci. Technol., B* **2003**, *21*, 148−155.
(45) Yamamoto, H.; Butera, R. A.; Gu, Y.; Waldeck, D. H. *Langmuir* **1999**, *15*, 8640−8644.
(46) Tanzer, T. A.; Bohn, P. W.; Roshchin, I. V.; Greene, L. H.; Klem, J. F. *Appl. Phys. Lett.* **1999**, *75*, 2794−2796.
(47) Sandroff, C. J.; Nottenburg, R. N.; Bischoff, J. C.; Bhat, R. *Appl. Phys. Lett.* **1987**, *51*, 33−35.
(48) Yablonovitch, E.; Sandroff, C. J.; Bhat, R.; Gmitter, T. *Appl. Phys. Lett.* **1987**, *51*, 439−441.
(49) Farrow, L. A.; Sandroff, C. J.; Tamargo, M. C. *Appl. Phys. Lett.* **1987**, *51*, 1931−1933.
(50) Bessolov, V. N.; Lebedev, M. V. *Semiconductors* **1998**, *32*, 1141−1156.
(51) Sheen, C. W. Quantitative analysis of molecular structure in monolayer thin films on nonmetallic substrates. The Pennsylvania State University, University Park, PA, 1993.
(52) Bain, C. D. *Adv. Mater.* **1992**, *4*, 591−594.
(53) Shi, J.; Hong, B.; Parikh, A. N.; Collins, R. W.; Allara, D. L. *Chem. Phys. Lett.* **1995**, *246*, 90−94.
(54) Remashan, K.; Bhat, K. N. *Thin Solid Films* **1999**, *342*, 20−29.
(55) Shaporenko, A.; Adlkofer, K.; Johansson, L. S. O.; Ulman, A.; Grunze, M.; Tanaka, M.; Zharnikov, M. *J. Phys. Chem. B* **2004**, *108*, 17964−17972.
(56) Lercel, M. J.; Tiberio, R. C.; Chapman, P. F.; Craighead, H. G.; Sheen, C. W.; Parikh, A. N.; Allara, D. L. *J. Vac. Sci. Technol., B* **1993**, *11*, 2823−2828.
(57) Lercel, M. J.; Craighead, H. G.; Parikh, A. N.; Seshadri, K.; Allara, D. L. *J. Vac. Sci. Technol., A* **1996**, *14*, 1844−1849.
(58) Lercel, M. J.; Rooks, M.; Tiberio, R. C.; Craighead, H. G.; Sheen, C. W.; Parikh, A. N.; Allara, D. L. *J. Vac. Sci. Technol., B* **1995**, *13*, 1139−1143.

tion to preparation and lab to lab, given the complicated surface chemistry of GaAs with respect to oxidation, effects of humidity, oxide removal,[41,51,59,60] and the natural tendency of the surface to reconstruct toward a more stable surface termination.[61,62] With these factors in mind we undertook a rigorously systematic study of preparation conditions, with a full set of characterization tools applied consistently to each type of preparation, to identify conditions which could lead to reproducibly dense, highly organized **ODT**/GaAs(001) SAMs.

In this report we show that such SAMs can be formed reproducibly under carefully controlled solution conditions if particular attention is paid to the control of humidity, removal of the native oxide, and rigorous use of anaerobic conditions to prevent regrowth during processing. Using infrared spectroscopy (IRS), near-edge X-ray adsorption fine structure (NEXAFS) spectroscopy, XPS, SWE, liquid drop contact angle measurements, and AFM, we show that highly conformal, organized SAMs can be formed with (1) near vertically oriented chains exhibiting high degrees of conformational ordering, (2) oxide free interfaces, (3) thermal stability up to ~100 °C, and (4) highly oleophobic surfaces indicative of dense, low defect ambient surfaces. Further, solution exposure experiments with deuterated **ODT** show the SAMs to be capable of a dynamic interchange of constituent molecules which allows insertion of selected molecules into the dense SAM structure, similar to the well-established insertion properties of alkanethiol SAMs on Au{111}.[63] Finally, analysis of the average molecular spacings, as deduced from the IR orientation data, combined with the presence of direct chemical bonding to the bare substrate, implies that the monolayers are incommensurate with the intrinsic (001) square lattice of the substrate.

2. Experimental Methods

2.1. Monolayer Formation: Definition of Standard Conditions for Maximum SAM Reproducibility, Stability, and Molecular Organization. Octadecane thiol (**ODT**), $CH_3[CH_2]_{17}SH$, and hexadecanethiol (**HDT**), $CH_3[CH_2]_{15}SH$, were obtained from Aldrich Chemical Co. (Milwaukee, WI). The synthesis of d_{37}-**ODT** was carried out following the procedure used by Fisher et al.[64] d_{37}-Bromooctadecane, as obtained from C/D/N ISOTOPES Inc. (Pointe-Claire, Quebec, Canada), was refluxed with an ethanolic solution of potassium thioacetate, and the resulting thioacetate was hydrolyzed with aqueous NaOH to obtain the corresponding sodium thiolate salt. d_{37}-**ODT** was obtained by the addition of degassed HCl to the sodium thiolate. Final purification of the thiol was achieved by flash chromatography with silica as the stationary phase and hexanes as the eluent. Purity of the synthesized d_{37}-**ODT** was shown to be >99% by GC/MS. n-Type (Si dopant, $0.8 \sim 4\times10^{18}/cm^3$) 2 in single side polished GaAs (001) wafers (American Xtal Technologies, Fremont, CA) were used for reflection IR; semi-insulating (S-I) wafer samples ($\sim 1 \times 1$ cm^2) were used for all other studies. No differences were observed between the SAM properties for doped and S-I wafers.

To determine the optimum procedure for preparing the best quality monolayers, a number of different conditions were used, including substrate cleaning procedures (ranging from acid to base etches), temperatures (ranging from ambient to 60 °C), solvents (including non-hydroxylic such as THF and hydroxylic such as ethanol), incubation times (ranging from minutes to days), and ambient atmospheres (including different humidities and control of O_2 concentration). Most of the conditions produced monolayers with irreproducible characteristics of typically poor quality and low stability to ambient exposure in terms of oxide growth at the interface. A narrow range of conditions, however, proved successful in providing highly reproducible monolayers with maximum degrees of organization and clean, stable interfaces with direct molecule−GaAs attachment. These conditions, termed our standard method, are described below and are the basis for all the characteristics reported throughout the paper unless otherwise stated.

The native oxide of GaAs was removed by immersing the substrates in concentrated NH_4OH (JT Baker, CMOS grade, 30% NH_4OH in water) from 1 to 5 min. The sample was rinsed with anhydrous ethanol (Pharmco, A.C.S./U.S.P. grade, degassed through multiple freeze−pump−thaw cycles) and dried with a N_2 stream, and SWE measurements were taken within 3 min. The substrates were then immediately immersed in degassed ethanolic solutions containing 3 mM **ODT** and ~10 mM NH_4OH and transferred into a nitrogen purged glovebox (O_2 < 5 ppm) for incubation for at least 20 h. The samples were removed from solution, dried with N_2, and removed from the glovebox for immediate characterization. We note that attempts to form a monolayer using this procedure with the pure, analogous disulfide, 1-octadecyldisulfanyl-octadecane, were unsuccessful; thus typical disulfide contaminants in the starting thiol have no effect on the preparations. Once complete analysis was done on a given sample, it was recycled for use by exposure to UV-ozone exposure to remove the monolayer and regrow an oxide layer. The oxide was subsequently removed by etching of NH_4OH. Use of recycled substrates gave identical results to those with fresh substrates. Reference samples made from **ODT** and hexadecanethiol (**HDT**) monolayers on Au surfaces were formed according to our standard protocol (e.g., see ref 64).

2.2. Infrared Spectroscopy. Spectra were collected using a custom, in-house modified Fourier transform spectrometer (BioRad FTS-7000/Digilab, Randolph, MA)[65] with sample−detector optics mounted on a goniometer and housed in an external N_2 or dry air (H_2O and CO_2 free) purge box. Both transmission (two-sided samples with a normal incidence IR beam) and reflection measurements (opaque, doped wafers) were made, but in general, better signal-to-noise spectra were obtained using reflection, so only these experimental conditions are described here. Spectra were obtained at 4 cm^{-1} resolution in order to avoid interference fringes that occur due to multiple back reflections (fringing) within the crystal faces of the GaAs wafers. Scans were collected at 20 kHz, and the interferograms were transformed using triangular apodization with zero filling for increased point density where needed. The incident beam was either *s* or *p* polarized and set at an 80° angle of incidence (AOI) from the surface normal. This angle gave the maximum signal-to-noise for a monolayer reflection spectrum over a range of AOI values from 50° to 86° as determined from the maximum value of the ratio of the intensity of the CH_2 *asym*, (d^-) peak located at 2917 cm^{-1} to the RMS peak-to-peak value of the baseline noise between 2500 and 2700 cm^{-1}, a featureless section of the monolayer spectrum.[66] Typically ~2000 scans were coadded to improve the signal-to-noise. Spectral intensities are reported as $-\log(I/I_0)$, where I is the output power of the IR beam from the samples and I_0 is the output power from a reference sample. The most useful reference was a bare GaAs substrate used immediately after oxide removal to minimize contamination.

(59) Chang, C. C.; Citrin, P. H.; Swartz, B. *J. Vac. Sci. Technol* **1977**, *14*, 943−952.
(60) Aspnes, D. E.; Studna, A. A. *Appl. Phys. Lett.* **1981**, *39*, 316−318.
(61) Xue, Q. K.; Hashizume, T.; Sakurai, T. *Prog. Surf. Sci.* **1997**, *56*, 1−131.
(62) Ranke, W.; Jacobi, K. *Prog. Surf. Sci.* **1981**, *10*, 1−52.
(63) Cygan, M. T.; Dunbar, T. D.; Arnold, J. J.; Bumm, L. A.; Shedlock, N. F.; Burgin, T. P.; Jones, L.; Allara, D. L.; Tour, J. M.; Weiss, P. S. *J. Am. Chem. Soc.* **1998**, *120*, 2721−2732.
(64) (a) Walker, A. V.; Tighe, T. B.; Haynie, B. C.; Uppili, S.; Winograd, S.; Allara, D. L. *J. Phys. Chem. B.* **2005**, *109*, 11263−11272. (b) Fisher, G. L.; Waltker, A. V.; Hooper, A. E., Tighe, T. T.; Bahnck, K. B.; Skriba, H. T.; Reinard, M. D.; Haynie, B. C.; Opila, R. L.; Winograd, N.; Allara, D. L. *J. Am. Chem. Soc.* **2002**, *124*, 5528−5541 and references therein.
(65) Parikh, A. N.; Allara, D. L. *J. Chem. Phys.* **1992**, *96*, 927−945.
(66) Data given in Supporting Information.

For thermal desorption measurements, the samples were mounted on a specially constructed holder consisting of a smooth copper plate resistively heated from the backside with heating tape. The sample temperature was monitored with a k-type thermocouple mounted to the front of the wafer under a spring clip. The temperature was controlled using a CN9000A Omega temperature controller (Omega Engineering, Inc. Stamford, CT). The sample was heated rapidly to the specified temperature within 1−3 min and held at that value within ±1 °C for the duration of the spectra acquisition, usually 10 min. The maximum temperatures that could be achieved with this experimental setup were between 483 and 493 K.

2.3. Spectral Simulations. Simulations of IR spectra for the **ODT** SAMs were modeled using a rigorous, full scale implementation of the 4 × 4 transfer matrix method developed by Yeh[67] and formulated by Parikh and Allara for organic thin film applications.[65] Since both parallel and perpendicular components of oscillators on GaAs can be excited,[68] all matrix elements of the optical function tensors were evaluated. For reflection spectra, the SAM structures were modeled as a uniaxially anisotropic SAM on an optically infinite, opaque isotropic substrate. The GaAs optical function spectra were obtained by interpolating values found from literature.[69] The SAM optical tensor spectra construction and corresponding best fit simulation procedures were done following our reported methods.[65] A series of calculations with an arbitrary SAM structure at a series of AOIs were run to help guide the selection of the optimum AOI in the experiments (see previous section and Supporting Information).

2.4. Near Edge X-ray Absorption Fine Structure (NEXAFS). The fabricated films were characterized by angle-resolved NEXAFS using the HE-SGM beamline of the synchrotron storage ring BESSY II in Berlin, Germany. The results were compared with the analogous data set for a hexadecanethiolate on Au{111} reference sample (**HDT**/Au). During analysis the samples remained at room temperature with a base pressure $< 1.5\times10^{-9}$ mbar. The spectra acquisition time was selected in such a way that no noticeable damage by the primary X-rays occurred during the measurements.[70−73]

Spectral acquisition was carried out at the C K-edge in the partial electron yield mode with a retarding voltage of −150 V. Linear polarized synchrotron light with a polarization factor of ∼82% was used. The energy resolution was ∼0.40 eV. The incidence angle of the light was varied from 90° (***E***-vector in surface plane) to 20° (***E***-vector near surface normal) in steps of 10°−20° to monitor the orientational order in the SAMs.

The raw spectra of **ODT**/GaAs and **HDT**/Au were normalized to the incident photon flux by division with a spectrum of a clean, freshly sputtered gold sample. In the case of **ODT**/GaAs, a raw spectrum of freshly sputtered GaAs was subtracted from the raw spectrum of a SAM-covered sample before the normalization, with both spectra being normalized to the pre-edge intensity.[26] The energy scale was referenced to the pronounced π^* resonance of highly oriented pyrolytic graphite at 285.38 eV.[74]

2.5. Other Measurements. Single wavelength ellipsometry (SWE) measurements were recorded using a Stokes ellipsometer (Gaertner Scientific Corporation, Skokie, Illinois) operating with a 632.8 nm beam set at a 70° angle of incidence. The experimentally measured polarization angles were used to determine film thickness using well-established modeling methods.[53,75] The ellipsometric parameters of the bare, freshly etched substrate were measured, and the pseudo-optical constant was calculated. Film thicknesses were then calculated from a two-layer SAM/substrate model in which the SAM complex refractive index is described as a scalar, $\hat{n} = n + ik$ and the substrate is assigned the measured pseudo-optical constant.

Contact angle measurements were made either using a Dynamic Wilhelmy balance (WB)[76,77] method with double side polished GaAs samples or sessile drop measurements (home-built apparatus with a CCD camera which captures drop images digitally). For the latter, the contact angles were analyzed using ImageJ software (National Institute of Health, USA). A 20 μL drop was dispensed on the surface with a flat tipped micrometer syringe (GS-1200, Gilmont Instruments, Barrington, IL) for each of the two probe liquids, Milli-Q water and hexadecane, HD (Sigma-Aldrich, 99+% anhydrous). The drop was then pulled across the surface at a rate of 50 μm/s using a piezo-electric micromanipulator to determine the advancing and receding angles. This method has been reported to return an angle somewhere between the max advancing angle and the equilibrium contact angle.[78] A minimum of three measurements were made at different spots for each sample, and at least three samples were tested for each probe liquid.

Tapping mode atomic force microscope imaging was performed with a Dimension 3100 scanning probe microscope (Digital Instruments, Santa Barbara, CA), using commercially available etched n-doped Si cantilevers, (20−80 N/m, Veeco, Santa Barbara, CA). Using the Digital Instrument software, roughness measurements were obtained from height images after a plane-fitting algorithm.

X-ray photoelectron spectroscopy (XPS) was performed with a monochromatic, Al Kα source instrument (Kratos, Axis Ultra; England) with a pass energy of 20 eV. In all cases, collection times were shorter than the onset of noticeable film degradation determined by comparing survey spectra before and after data collection. Data were collected with photoelectron take off angles of 60° and 90° from the surface normal. All spectra were referenced to the As 3d 5/2 peak at 40.95 eV.

3. Results and Discussion

3.1. Monolayer Structure. 3.1.1. Surface Topography by Tapping Mode AFM. Direct comparison of the images in Figure 1 shows no discernible changes in the surface topography of a typical GaAs(001) substrate as received, after the NH_4OH oxide etching step and after formation of an **ODT** SAM. The corresponding rms roughnesses are 3.9, 3.9, and 3.7 Å, respectively. Neither the bare (with the native oxide layer) nor the oxide-etched wafer exhibit any features of the underlying crystal structure such as terraces or aligned step edges. Similar topography has been observed for GaAs(001) surfaces by scanning tunneling microscopy when the native oxide was removed using NH_4OH.[79−81] These data show that our standard **ODT** assembly process does not roughen the initial substrate topography and produces highly conformal SAMs.

3.1.2. Monolayer Wetting Properties. The Wilhelmy method gives advancing contact angle (θ_a) and associated hysteresis values ($\Delta\theta$) of 115 ± 2°, 11 ± 1° and 44 ± 1°, 4 ± 1° for H_2O and hexadecane (HD), respectively. Sessile drop measurements

(67) Yeh, P. *Optical Waves in Layered Media*; Wiley-Interscience: New York, 1988.
(68) Hecht, E. *Optics*, 4th ed.; Adison Wesley: 2001.
(69) Palik, E. D. *Handbook of Optical Constants*; Academic Press: New York, 1985.
(70) Wirde, M.; Gelius, U.; Dunbar, T.; Allara, D. L. *Nucl. Instrum. Methods Phys. Res., Sect. B* **1997**, *131*, 245−251.
(71) Jager, B.; Schurmann, H.; Muller, H. U.; Himmel, H. J.; Neumann, M.; Grunze, M.; Woll, C. *Z. Phys. Chem.* **1997**, *202*, 263−272.
(72) Heister, K.; Zharnikov, M.; Grunze, M.; Johansson, L. S. O.; Ulman, A. *Langmuir* **2001**, *17*, 8−11.
(73) Zharnikov, M.; Grunze, M. *J. Vac. Sci. Technol., B* **2002**, *20*, 1793−1807.
(74) Batson, P. E. *Phys. Rev. B* **1993**, *48*, 2608−2610.
(75) Collins, R. W.; Kim, Y. T. *Anal. Chem.* **1990**, *62*, A887.
(76) Lander, L. M.; Siewierski, L. M.; Brittain, W. J.; Vogler, E. A. *Langmuir* **1993**, *9*, 2237−2239.
(77) Vogler, E. A. *Langmuir* **1992**, *8*, 2013−2020.
(78) Bain, C. D.; Troughton, E. B.; Tao, Y. T.; Evall, J.; Whitesides, G. M.; Nuzzo, R. G. *J. Am. Chem. Soc.* **1989**, *111*, 321−335.
(79) Wang, X. S.; Self, K. W.; Maboudian, R.; Huang, C.; Bresslerhill, V.; Weinberg, W. H. *J. Vac. Sci. Technol., A* **1993**, *11*, 1089−1093.
(80) Khatiri, A.; Ripalda, J. M.; Krzyzewski, T. J.; Bell, G. R.; McConville, C. F.; Jones, T. S. *Surf. Sci.* **2004**, *548*, L1−L6.
(81) Sonnenfeld, R.; Schneir, J.; Drake, B.; Hansma, P. K.; Aspnes, D. E. *Appl. Phys. Lett.* **1987**, *50*, 1742−1744.

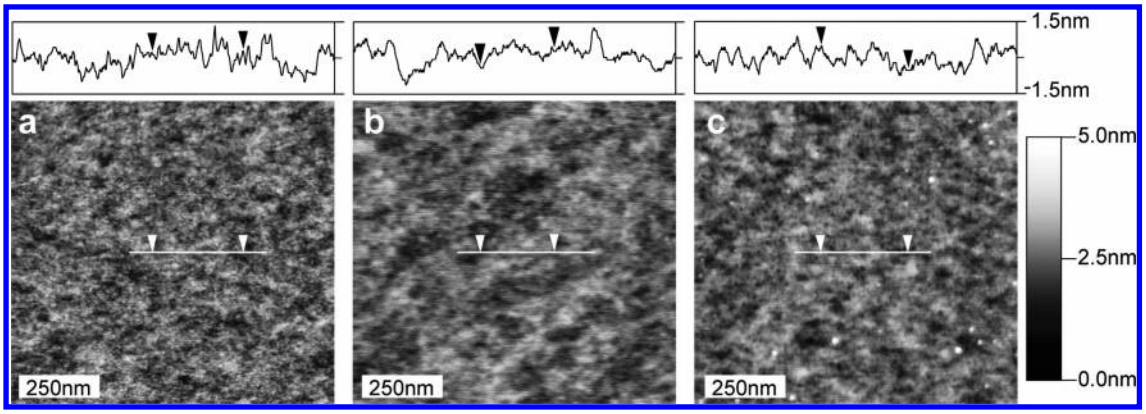

Figure 1. AFM tapping mode topography of the GaAs(001) surface: (a) starting native oxide covered substrate, (b) after NH_4OH etching, (c) after **ODT** monolayer assembly.

give respective θ_a and $\Delta\theta$ values of 111 ± 3°, 16 ± 4° and 43 ± 1°, 2 ± 1°. The generally higher values of contact angles from the Wilhelmy method have been observed previously.[76] Both sets of data indicate highly hydrophobic and oleophobic monolayers, similar to the characteristics of long chain alkanethiolate SAMs on metal surfaces.[82] For example, for comparison with **ODT**/Au{111} SAMs prepared in our own lab and measured by the sessile drop method, we typically obtain advancing water and hexadecane contact angles in the range of ~110−115° and ~43−45 ± 1° with ~10° and ~4 ± 1° hysteresis, respectively. The appearance of contact angle hysteresis has been ascribed to various effects, including surface roughness, surface heterogeneity, liquid penetration and swelling effects, all of which in one form or another relate to surface defects in the molecular packing.[83,84] Although the **ODT**/GaAs SAMs exhibit a smooth surface (~4 Å RMS roughness, see Figure 1), quite close to the roughness observed for alkanethiolate SAMs on ultra flat gold surfaces,[85] hysteresis is not observed for the latter.[85,86] In addition, well formed octadecylsiloxane ($C_{18}H_{37}SiO_2$; OTS) SAMs on SiO_2 show no measurable hysteresis for hexadecane contact angles.[87] These comparisons suggest that the **ODT**/GaAs SAM has additional degrees of surface defects, arising from some combination of molecular organization and substrate topography.

3.1.3. Molecular Chain Tilt from NEXAFS. Carbon K-edge NEXAFS spectra of **ODT**/GaAs SAMs acquired at X-ray incident angles of 90°, 55°, and 20° are presented in Figure 2, along with the difference between the 90° and 20° spectra. The spectra exhibit a C 1s absorption edge related to C 1s → continuum excitations and all characteristic absorption resonances of extended alkyl chains in an all-*trans* conformation, namely a sharp resonance at ~287.7 eV and two broader resonances at ~293.4 eV and ~301.6 eV. The former resonance, denoted as R*, is attributed to mixed valence Rydberg states[88−90]

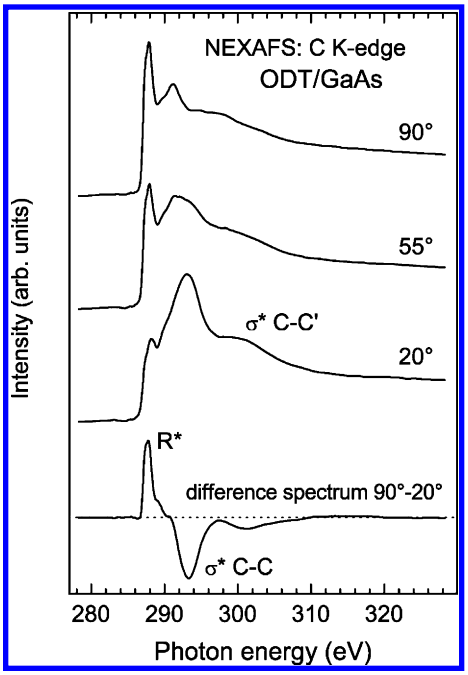

Figure 2. C K-edge NEXAFS spectra of **ODT**/GaAs acquired at X-ray incidence angles of 90°, 55°, and 20°, along with the respective difference spectra. The spectra are normalized to the height of the absorption edge. The characteristic absorption resonances are marked.

with a dominance of Rydberg states,[91,92] while the two latter resonances are commonly related to valence, antibonding C−C σ^* and C−C′ σ^* orbitals.[88,93] The molecular orbitals related to the R* resonance are oriented perpendicular to the alkyl chains,[93−96] whereas the transition dipole moments of the orbitals corresponding to the C−C σ^* and C−C′ σ^* resonances are directed along the chain axis.[94,95] Thus, the orientations of these orbitals unequivocally determine the orientation of the alkyl chains in the SAMs.

The spectra exhibit a pronounced dependence of the absorption resonance intensity on the incidence angle of X-rays, which

(82) Laibinis, P. E.; Whitesides, G. M.; Allara, D. L.; Tao, Y. T.; Parikh, A. N.; Nuzzo, R. G. *J. Am. Chem. Soc.* **1991**, *113*, 7152−7167.
(83) Kwok, D. Y.; Neumann, A. W. *Adv. Colloid Interface Sci.* **1999**, *81*, 167−249.
(84) Lam, C. N. C.; Wu, R.; Li, D.; Hair, M. L.; Neumann, A. W. *Adv. Colloid Interface Sci.* **2002**, *96*, 169−191.
(85) Gupta, P.; Loos, K.; Korniakov, A.; Spagnoli, C.; Cowman, M.; Ulman, A. *Angew. Chem., Int. Ed.* **2004**, *43*, 520−523.
(86) Gupta, P.; Ulman, A.; Fanfan, S.; Korniakov, A.; Loos, K. *J. Am. Chem. Soc.* **2005**, *127*, 4−5.
(87) Parikh, A. N.; Allara, D. L.; Azouz, I. B.; Rondelez, F. *J. Phys. Chem.* **1994**, *98*, 7577−7590.
(88) Stohr, J. *NEXAFS Spectroscopy;* Springer-Verlag: Berlin, 1992.
(89) Vaterlein, P.; Fink, R.; Umbach, E.; Wurth, W. *J. Chem. Phys.* **1998**, *108*, 3313−3320.
(90) Scholl, A.; Fink, R.; Umbach, E.; Mitchell, G. E.; Urquhart, S. G.; Ade, H. *Chem. Phys. Lett.* **2003**, *370*, 834−841.
(91) Bagus, P. S.; Weiss, K.; Schertel, A.; Woll, C.; Braun, W.; Hellwig, C.; Jung, C. *Chem. Phys. Lett.* **1996**, *248*, 129−135.
(92) Weiss, K.; Bagus, P. S.; Woll, C. *J. Chem. Phys.* **1999**, *111*, 6834−6845.
(93) Outka, D. A.; Stohr, J.; Rabe, J. P.; Swalen, J. D. *J. Chem. Phys.* **1988**, *88*, 4076−4087.
(94) Hahner, G.; Kinzler, M.; Woll, C.; Grunze, M.; Scheller, M. K.; Cederbaum, L. S. *Phys. Rev. Lett.* **1991**, *67*, 851−854.
(95) Hahner, G. *Phys. Rev. Lett.* **1992**, *69*, 694.
(96) Hahner, G.; Kinzler, M.; Thummler, C.; Woll, C.; Grunze, M. *J. Vac. Sci. Technol., A* **1992**, *10*, 2758−2763.

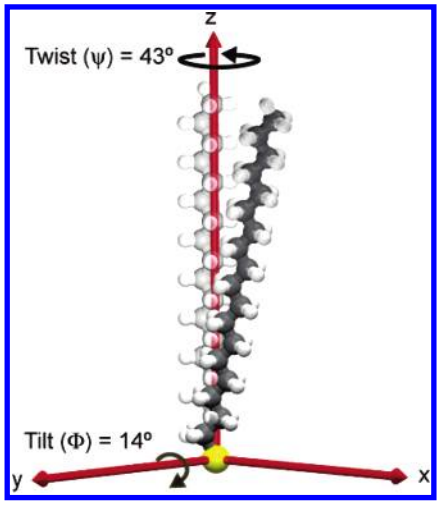

Figure 3. A representation of an **ODT** molecule oriented in a coordinate system in which the $x-y$ plane represents the GaAs substrate surface. The molecule is initially oriented with the C−C−C backbone in the $x-z$ plane. The final configuration is defined by a twist (ψ) about the z-axis and a tilt (Φ) around the y-axis in the $x-z$ plane. The best fit values of the angles from NEXAFS and IR are indicated.

suggests a high orientational order in these SAMs. Considering the transition dipole moment directions of the R*, C−C σ*, and C−C′ σ* orbitals and the character of the observed intensity changes, an upright orientation of the alkyl chains can be assumed. To determine the specific value of the average chain orientation, a quantitative analysis was performed by measuring the intensity of the R* resonance as a function of the X-ray incidence angle, θ. The resulting dependence was then evaluated according to theoretical expressions (for a plane-type orbital)[88]

$$I(\gamma,\theta) = A\left\{P \times \frac{2}{3}\left[1 - \frac{1}{4}\cdot(3\cdot\cos^2\theta - 1)\cdot(3\cdot\cos^2\gamma - 1)\right] + (1-P)\times\frac{1}{2}\cdot(1+\cos^2\gamma)\right\}, \quad (1)$$

where A is a constant, P is a polarization factor of the X-rays, and γ is the angle between the sample normal and the normal of the molecular orbital plane. The intensity ratios $I(\theta)/I(20°)$ were then analyzed,[88] where $I(\theta)$ and $I(20°)$ are the intensities of the R* resonance at X-ray incidence angles of θ and 20° (see Supporting Information). The results yield an average alkyl chain tilt angle (Φ) of 14.9° for the **ODT**/GaAs SAM, where the tilt angles are as defined in Figure 3, while the analogous value for the **HDT**/Au SAM was found to be 30°, in good agreement with literature data.[88,92−95] The accuracy of these values is ±3°−5°, which is just a general accuracy of the NEXAFS experiment and data evaluation procedure.

In addition to the above standard evaluation procedure, we processed the NEXAFS data using difference spectra, as presented in Figure 2. As described elsewhere,[88] upon subtracting two NEXAFS spectra recorded at different X-ray incidence angles θ and θ_1, one obtains

$$I_v(\theta) - I_v(\theta_1) = C_v(1 - {}^3/_2\cdot\sin^2\alpha)(\cos^2\theta - \cos^2\theta_1) \quad (2)$$

$$I_p(\theta) - I_p(\theta_1) = C_p(1 - 3\cdot\cos^2\gamma)(\cos^2\theta - \cos^2\theta_1) \quad (3)$$

for a vector (v) and a plane (p) and orbital, respectively. $I_{v/p}(\theta)$ and $I_{v/p}(\theta_1)$ are the resonance intensities, α is the angle between the sample normal and the transition dipole moment of the vector orbital, and $C_{v/p}$ is a normalization constant, which depends on the excitation probability from the C 1s core level into a given molecular orbital.

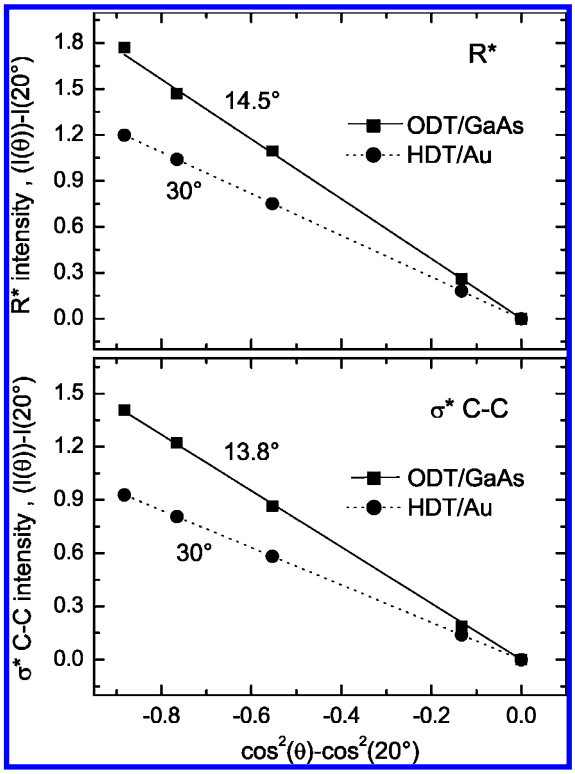

Figure 4. Plots of the intensities of the R* (upper panel) and σ* C−C (bottom panel) difference peaks for **ODT**/GaAs (■) and **HDT**/Au (●) versus $\cos^2\theta - \cos^2(20°)$ along with the respective linear fits (solid and dashed lines, respectively) using least-squares analysis. The derived average alkyl chain tilt angles (Φ) are given at the respective fits. The data for **HDT**/Au are given for comparison. See text for details.

Plots of difference peak intensities of the R* and σ* C−C resonances for **ODT**/GaAs and **HDT**/Au versus $\cos^2\theta - \cos^2\theta_1$ show highly linear dependencies (Figure 4) from which the slopes yield $C_v(1-{}^3/_2\cdot\sin^2\alpha)$ and $C_p(1-3\cdot\cos^2\gamma)$ for the σ* C−C and R* resonances, respectively. Defining the chain tilt angle as shown in Figure 3 and assuming 30° as the average tilt angle of the alkyl chains in the **HDT**/Au SAM,[88,93−96] we calculate C_v and C_p for the **ODT**/GaAs SAM and obtain average chain tilt angle values of 13.8° and 14.5° on the basis of the $\alpha(\sigma$* C−C) and γ(R*) values, respectively. Both these values are in excellent agreement with a value of 14.9° obtained by the standard evaluation of the NEXAFS data (see above). Taking the average over all three values, we determine 14.4° for the average tilt angle of the alkyl chain in the **ODT**/GaAs SAM.

The nearly perpendicular molecular tilt angle of 14° derived from our NEXAFS measurements is strikingly different from the 57° tilt angle reported originally for **ODT** monolayers on GaAs(001)[23] prepared from molten thiol at 100 °C and indicates that this original preparation produces a different structure than the present, room temperature solution method. The 14° angle is similar to the chain cants reported for alkanethiols assembled on evaporated Ag{111} and Cu{111} metal surfaces (∼12°)[82] and also to OTS films on SiO_2 (∼10°).[87] In contrast, alkanethiols on Au{111} surfaces exhibit a significantly higher average tilt

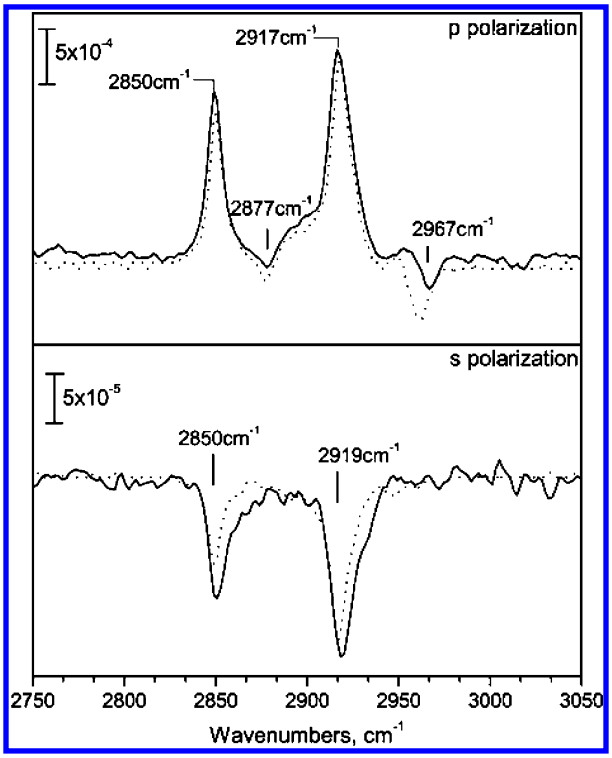

Figure 5. IR reflection spectra (80° angle of incidence) of the C−H stretching region for an **ODT** monolayer on GaAs (001). (Top) *p* polarized spectrum; (Bottom) *s* polarized spectrum. For both spectra the solid and dotted lines denote the experimental and best-fit simulated spectra, respectively. The best fit simulation corresponds to a chain model with tilt and twist angles of 15° and 43°, respectively.

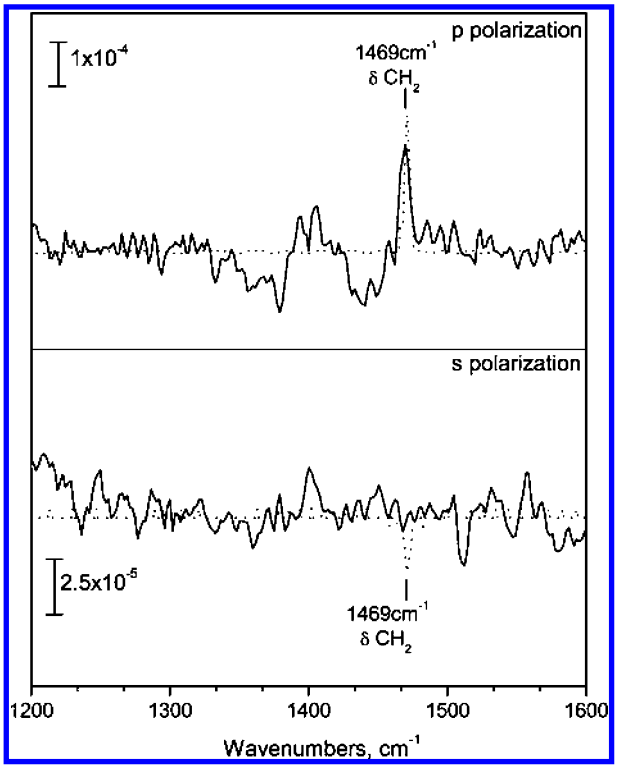

Figure 6. IR reflection spectra (80° angle of incidence) of the low-frequency region for an **ODT** monolayer on GaAs (001). (Top) *p* polarized spectrum; (Bottom) *s* polarized spectrum. For both spectra the solid and dotted lines denote the experimental and best-fit simulated spectra, respectively. The simulated spectra are based on the same chain model as that in the C−H stretching mode simulations (see previous figure).

angle of ∼30°.[97] A full discussion of the implications of the molecular tilt angle for the **ODT**/GaAs SAM structure is deferred to a later section.

3.1.4. Monolayer Thickness. Given the 14 ± 2° chain tilt angle from NEXAFS measurements and a physical length of ∼24.5 Å for a fully extended $C_{18}H_{37}S$−thiolate moiety bonded at the GaAs surface, we set the physical thickness of the **ODT**/GaAs SAM at 23.8 ± 0.2 Å. In contrast, a value of 21 ± 2 Å is obtained from our SWE measurements when interpreted using an isotropic model with an overall refractive index of 1.50 for the alkanethiolate moiety.[53] We regard the NEXAFS derived value as more reliable for two reasons. First, the NEXAFS analysis of the **HDT**/Au{111} SAM gives tilt angles that match those from a variety of other methods quite closely (see above), thus implying that the tilts for the **ODT**/GaAs SAM are accurate. Second, the assumption of $n = 1.50$ for the monolayer film is based on the value assigned to the **ODT**/Au{111} SAM which includes the contribution of a S−Au interface layer.[53] One can expect that a different interface layer contribution is required for the **ODT**/GaAs SAM to account for the specific electronic character of the S−(GaAs) region of the film. To obtain accurate SWE thickness values, a more complex model that accounts for the influence of the GaAs−thiol interface on the optical properties needs to be developed (e.g., via spectroscopic ellipsometry[53]).

3.1.5. Chain Conformational Ordering from IRS. Reflection spectra for both *p* and *s* polarized light are shown in Figures 5 and 6. Transmission spectra also were recorded but are not shown since they are less informative. The presence of both positive and negative absorbance features in the reflection spectra result from well-known effects involving strong perturbations of the electric fields by the real part of the optical functions of the film in the case of dielectric substrates.[65] For simple first-order ***E***-field responses at angles greater than Brewster's angle, as is the case in these experiments, negative peaks result in the *s* polarized spectrum, while positive or negative peaks result in the *p* polarized spectrum according to whether the transition dipoles of the oscillators are oriented parallel or perpendicular to the substrate, respectively.[65,98−100]

The peaks can be assigned readily by comparison with previous work on alkanethiolate SAMs/Au:[82] 2850 cm^{-1} [C−H methylene *sym.* str. (d^+)], 2877 cm^{-1} [C−H methyl *sym.* str. (r^+) split by Fermi Resonance (FR) interaction with the CH_3 *asym.* def.[101]], 2917 cm^{-1} [*antisym.* str. (d^-)], and 2967 cm^{-1} [methyl *asym.* in-plane str. (r_a^-)]. The appearance of the *sym.* and *antisym.* C−H methylene str. modes at 2950 and 2917 cm^{-1} indicates a high degree of conformational ordering of the alkyl chains, closely comparable to that in **ODT**/Au{111} SAMs for which the above modes appear at the same frequencies.[82] The peak assignments are summarized in Table 1 for reference.

In the low-frequency region of the *p* polarized spectrum (Figure 6), the peak observed at 1469 cm^{-1} is assigned to the methylene scissor deformation mode (δ CH_2). No obvious splitting is seen within the resolution and signal/noise of our

(97) Sellers, H.; Ulman, A.; Shnidman, Y.; Eilers, J. E. *J. Am. Chem. Soc.* **1993**, *115*, 9389−9401.
(98) Berreman, D. W. *Phys. Rev.* **1963**, *130*, 2193-2198.
(99) Yen, Y. S.; Wong, J. S. *J. Phys. Chem.* **1989**, *93*, 7208−7216.
(100) Supporting Information.
(101) Hill, I. R.; Levin, I. W. *J. Chem. Phys.* **1979**, *70*, 842−851.

Table 1. IRS Peak Positions and Mode Description of **ODT** Monolayers on GaAs (001)

	frequency, cm^{-1}			
	obsd	calcd[a]	description of mode[b]	intensity[c]
p polarization	2967	2961	CH_3 *asym*, (ip), (r_a^-)	+, m
		2949	CH_3 *asym*, (r_b^-)	+, w
	2917	2917	CH_2 *asym*, (d^-)	+, m
		2937	CH_3 *sym*, (r^+, FR)	−, vw
	2877	2876	CH_3 *sym*, (r^+, FR)	−, w
		2895	CH_2 *sym*, (d^+, FR)	+, w
	2850	2850	CH_2 *sym*, (d^+)	+, s
	1469	1469	CH_2 scissors def, δ CH_2	+, w
	1383		CH_3 def (*sym*), δ CH_3	
s polarization		2961	CH_3 *asym*, (ip), (r_a^-)	−, vw
		2948	CH_3 *asym*, (r_b^-)	−, w
	2917	2917	CH_2 *asym*, (d^-)	−, vs
		2877	CH_3 *sym*, (r^+, FR)	−, vw
		2898	CH_2 *sym*, (d^+, FR)	−, w
	2850	2850	CH_2 *sym*, (d^+)	−, s
	1469	1469	CH_2 scissors def, δ CH_2	−, w

[a] Peak positions were determined from simulations of each individual mode; see Supporting Information. [b] Abbreviations used: *asym* = asymmetric or antisymmetric, *sym* = symmetric, ip = in plane, FR= Fermi resonance, def= deformation, sh = shoulder. [c] The intensity and its direction are based on calculations of each single mode. + = positive direction, − = negative direction, vs = very strong, s = strong, w = weak, vw = weak.

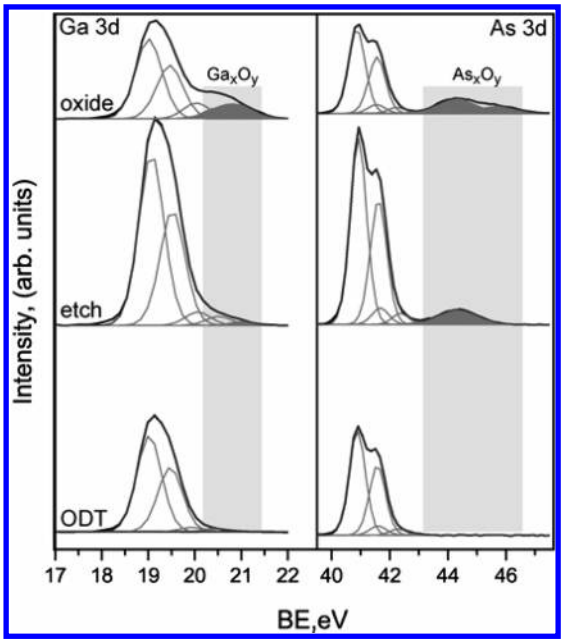

Figure 7. Comparison of the Ga 3d and As 3d region XPS spectra of the starting native oxide on GaAs (001) (top), after NH_4OH etching (middle), and after formation of the **ODT** monolayer (bottom). All spectra were taken with a 90° photoelectron takeoff angle.

spectra. Splitting has been noted to occur in this mode for close-packed polymethylene chains in a 2 chain/unit subcell in an orthorhombic packing crystal structure.[102] While this type of structure arises in alkanethiolate/Au{111} SAMs,[82] splitting of this mode has been observed only at low temperatures (e.g., for the $C_{22}H_{45}S$-/Au{111} SAM[103]). Other peaks expected in this region, based on the spectra of alkanethiolate/Au{111} SAMs, include the CH_3 deformation mode (δ CH_3) at ~1383 cm^{-1} and the wag/twist progression in the 1150−1350 cm^{-1} region. It is likely that we could not observe these features based on the lower signal-to-noise inherent in our spectra for a dielectric substrate, relative to the typical case of a highly reflective metal such as gold, and the intrinsic weak intensities of these peaks.

3.1.6. Molecular Orientation from IRS. Simulations of IR spectra were carried out for an air/SAM/GaAs sample with oriented chains. The thickness of the SAM layer was set at the NEXAFS derived value of 23.8 ± 0.2 Å, and previously determined optical tensor spectra for polycrystalline octadecanethiol were used to describe the optical response of the SAM.[65] The GaAs optical function spectra were obtained from the literature.[69] Presuming fully extended all-*trans* chains, simulations were carried out for a range of chain tilt and twist angles (see Figure 3) until best fits were achieved. The best fit results for the C−H stretching mode region, shown in Figure 5 as dotted lines, were obtained with chain tilt (Φ) and twist (ψ) angles 15 ± 1° and 43 ± 1°, respectively. Given the various sources of experimental error we set a conservative value of the twist at 43 ± 5°. The chain tilt is in excellent agreement with the NEXAFS derived value of 14 ± 2° and shows that the thickness and molecular orientation data are self-consistent. The results of these best fit conditions for simulation of the low frequency region are shown in Figure 6. The only observable peak, the CH_2 bending mode, shows a good fit in the *p* polarized spectrum but not in the *s* case. The latter spectrum, however, is at the edge of the noise limit making quantitation problematic. The best-fit conditions also yield simulated CH_3 bending and progression modes intensities below the noise limit. Further details of the simulations are given in the Supporting Information.

3.2. Molecule−Substrate Bonding by XPS. The effect of the **ODT** monolayers on the GaAs surface chemical states was determined from XPS measurements. In Figure 7, a comparison of the Ga 3d and As 3d regions is made for GaAs(001) samples with the native oxide present, freshly etched by NH_4OH, and modified by formation of an **ODT** monolayer. To obtain the etched surface spectrum, the GaAs(001) surface was etched under normal conditions (see Experimental Section), removed, rinsed, and transferred within 1−3 min into the XPS instrument where it was immediately exposed to vacuum. Since these conditions mimic the length of time that the etched substrate is exposed to ambient conditions (for SWE measurements) before immersion into the **ODT** solution, the amount of oxidation present in the NH_4OH etch spectrum is likely very similar to the amount of oxidation on the substrate when immersed in solution. The main Ga 3d and As 3d peaks were fit self-consistently with a series of doublets. The oxidized components (As_xO_y and Ga_xO_y, shaded in gray in Figure 7.) were fit with only single peaks due to the inherent broad shapes and the uncertainty in the specific components of the native oxide on GaAs. For both the Ga 3d and As 3d regions for all three samples, two doublets each were fit to the peaks, assigned as the contributions from bulk Ga (19.0 eV) or As (40.9 eV) species and surface Ga (20.0 eV) or As (41.6 eV) species. No specific peaks for As−S or Ga−S binding could be resolved in the monolayer spectra.

The spectra show a significant reduction in the amount of surface oxide after etching. The residual oxide could arise from

(102) Snyder, R. G.; Hsu, S. L.; Krim, S. *Spectrochimica Acta* **1978**, *34A*, 395−406.
(103) Nuzzo, R. G.; Korenic, E. M.; Dubois, L. H. *J. Chem. Phys.* **1990**, *93*, 767−773.

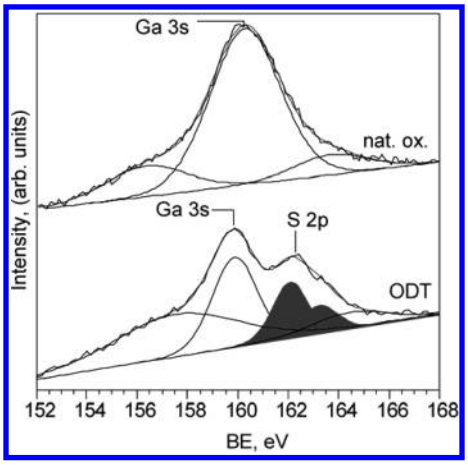

Figure 8. Comparison of the Ga 3s and S 2p region XPS spectra of the native oxide of GaAs (001) and the **ODT** modified surface. The spectra were taken with a 60° photoelectron takeoff angle. See text for details.

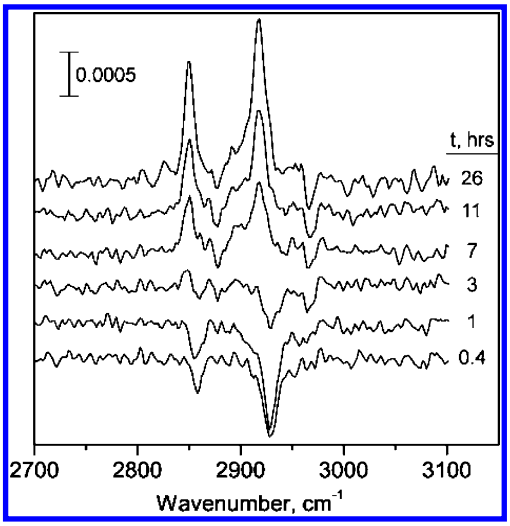

Figure 9. A series of *p* polarized IRS spectra of the C−H stretching region of the **ODT**/GaAs (001) SAM taken at room temperature (293 K) and after sequentially heating to 313, 353, 393, and 483 K. The spectrum after cooling back to room temperature (293 K*) is also shown. See text for details.

incomplete etching and/or the brief exposure to ambient. After formation of the **ODT** monolayer, however, no oxide surface species are observed.[104] Oxide removal could arise during SAM formation via etching by the NH_4OH in the thiol solution and/or a sacrificial chemical removal by the solute thiol. Since good quality monolayers can be formed, however, without addition of the NH_4OH, albeit with less reproducibility, it is likely that the thiol is the main agent for oxide removal.

Comparison of the S 2p and Ga 3s core level spectra for the native oxide and the SAM is given in Figure 8. The spectra were curve fit to show the contributions of the component features. In the native oxide spectrum while the Ga 3s peak (160 eV) dominates the contributions, two As 3p plasmon features are required to obtain good fits. In the SAM spectrum the additional doublet at 162.0 eV can be ascribed to a S 2p feature arising from a thiolate species,[55] consistent with a direct S−substrate bonding. Limitations in the signal-to-noise and instrumental resolution preclude further resolution of the thiolate peaks into specific components due to Ga−S and/or As−S species and thus make assignments of the specific SAM−substrate binding chemistry problematic. This uncertainty, in turn, affects other characterizations such as determinations of the monolayer thickness based on (C 1s)/(Ga 3d) and (C 1s)/(As 3d) peak area intensity ratios.[104]

Testing of the resistance of these SAMs to reoxidation of the underlying substrate was carried out at 1, 2, and 4 week intervals for sets of freshly made films stored at room temperature under normal laboratory conditions. The samples remained oxide free at least up to a month with some variations, but all samples showed a complete absence of oxide for up to 2 weeks of storage time. After this time, reoxidation of the underlying substrate was by appearance of the As_xO_y and Ga_xO_y peaks, but only 3% of the total As 3d signal and 2% of the Ga 3d signal was assigned to these components. This is in comparison to the native oxide where 14% of the As 3d signal and 7% of the Ga 3d signal were attributed to As_xO_y and Ga_xO_y peaks, respectively. Presumably the variations in the time for oxide formation are due to subtle differences in defect contents in the films. A comparison of the As 3d and Ga 3d core level spectra for these SAMs is included in the Supporting Information.

3.3. Monolayer Dynamic Properties. 3.3.1. Temperature Programmed Desorption (TPD) by IRS. The stability of the **ODT**/GaAs SAM under a nitrogen atmosphere at a series of temperatures from ambient to 483 K (210 °C) and back to ambient was followed by tracking the IR spectra in the C−H stretching region. The spectra are shown in Figure 9, and the intensity and frequency variations of the d^- peaks are shown in Figure 10.[105] Also shown are comparison data for a **ODT**/Au{111} SAM.

Up to temperatures of 353 K, very little change in the C−H peaks is observed for the GaAs SAM. The frequencies show a small positive shift with increasing temperature, and the intensities decrease slightly. Between 353 and 393 K, however, strong changes arise. Relative to the 353 K spectra, at 393 K the d^- peak is shifted by $\sim$+9 cm^{-1} (Figure 10, bottom) and both the d^- and d^+ peaks are inverted from positive to negative intensities (Figure 10, top). The large positive frequency shifts can be interpreted in terms of a severe decrease in conformational ordering of the chains, approaching the average defect density in a constrained liquid state. The intensity inversions can be understood on the basis of anisotropic refractive index tensor effects that arise from changes in the orientation of the alkyl chains. Simulations of the spectra for different tilt angles of an average extended *trans*-conformation chain predict that intensity flipping of the above modes will occur when the average tilt angle increases above $\sim$45°. Given the extensive disordering of the chains, however, it is not possible to accurately define orientation angles in terms of a well-defined chain vector, and thus more accurate simulations were not pursued. Overall we conclude that the chains adopt average orientations much more parallel to the surface than those for the original SAM. In a separate experiment the sample was

(104) A small tail on the high binding energy region of both the Ga 3d and As 3d regions could be attributed to either the inelastic collision of photoelectrons or to a trace amount of oxidation remaining on the substrate. Both higher resolution XPS experiments and time-of-flight secondary mass spectrometry measurements are currently underway to further examine the completeness of oxide removal. In addition these experiments will probe more deeply into the nature of the S−(GaAs) interface bonding.

(105) We report only the TPD IRS spectra with *p*-polarized light. The *s* polarized spectra are an order of magnitude weaker and, when combined with thermal instabilities in the baseline during heating, make interpretation somewhat problematic, particularly at the higher temperatures where short scan times are needed to obtain data during rapid changes in the SAMs.

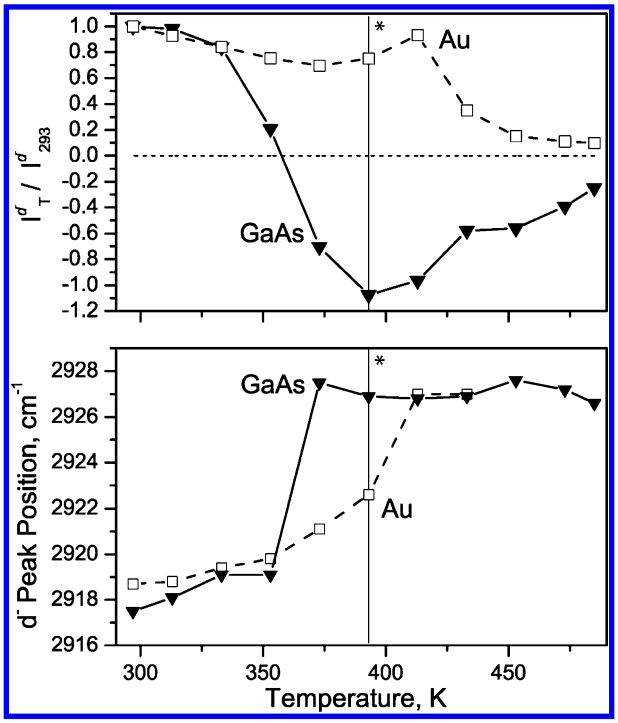

Figure 10. (Top) A comparison of the fractional change in intensity of the d^- peak intensity from *p* polarized IRS spectra of **ODT** SAMs on GaAs (001) and Au{111} as a function of increasing temperature. The horizontal dotted line represents complete loss of intensity which is associated with complete desorption. (Bottom) The corresponding comparison of the change in the d^- peak positions. The vertical line marked with an asterisk in both plots is at 393 K. See text for details.

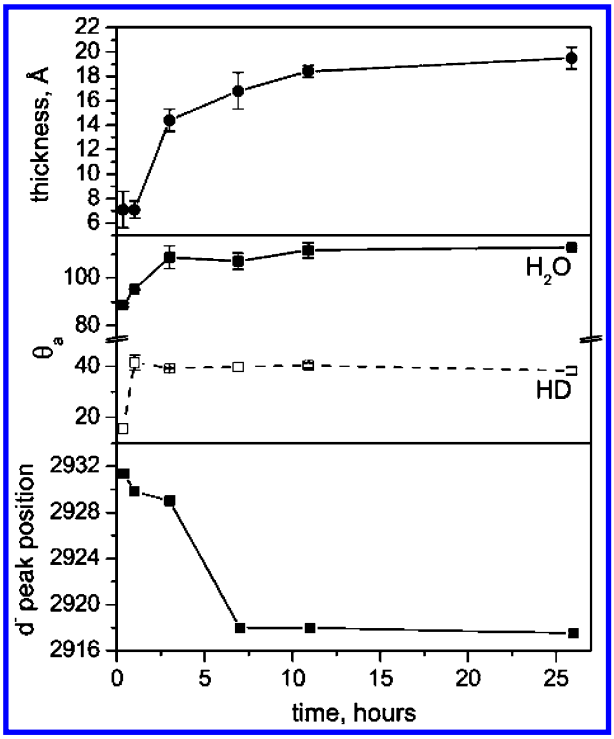

Figure 11. Dynamics of the adsorption of **ODT** monolayers from ethanol on GaAs. Lines are drawn as a guide to eye. (Top) Ellipsometric thickness. (Middle) Advancing contact angles of H_2O (filled squares) and hexadecane (open squares). (Bottom) The change in the d^- peak position as a function of time; see text for details.

heated in exactly the same way as above but cooled to room temperature once the 393 K data had been taken. The final room temperature IR spectrum was weaker and altered from the original (data not shown; see Supporting Information). The loss of a fraction of the adsorbed molecules is indicated by the SWE film thickness decrease to ~15 Å and a small reduction in the C 1s XPS signal (data not shown). The decrease in coverage is consistent with increased chain tilts and disorder, since in an initially densely packed monolayer space must be created to allow chains to assume larger tilt angles. Presuming that adsorbate desorption occurs randomly across the surface, the organization of the chains will irreversibly diminish with permanent loss in the average chain conformational ordering.

Once a GaAs SAM is raised above 393 K a continual reduction in the peak intensities becomes the dominant feature (Figures 9 and 10). Finally, after cooling back to ambient temperature the spectrum (indicated by an asterisk in Figure 9) remains inverted with very weak intensities. This observation indicates that considerable material has been desorbed and the remaining adsorbate molecules continue to be significantly disordered and lie closer to the surface on average. In agreement, the SWE film thickness is diminished to <5 Å, and the C 1s XPS signal is strongly reduced (data not shown).

It is instructive to compare these observations with corresponding TPD data for the SAM on Au{111}. Previous work has shown that in the region of ~393 K **ODT**/Au SAMs undergo a structural transition with a softening of the chain conformational ordering.[103,106] Our own data show (Figure 10, top) that the d^- peak intensity for the Au SAM drops off initially with increasing temperature and then somewhat levels off in the region of ~375−425 K. In parallel, peak broadening occurs (Figure 10, bottom), which correlates with the expected increases in chain disordering.[107] The final decrease in intensity is associated with the loss of adsorbate species from the surface. In contrast, the **ODT**/GaAs SAM peak frequency trends with *T* show that the alkyl chains start to undergo conformational disorder at lower temperatures than those for the Au SAM. Similar to the Au SAM, once the GaAs SAM reaches a state of limiting film disorder, the adsorbates begin to desorb irreversibly.[108]

3.3.2. Monolayer Formation Rates. The time evolution of **ODT**/GaAs SAM characteristics during film assembly was followed by immersing multiple wafers in the same thiol solution in the glovebox and removing a given sample for each time measurement. The contact angle and SWE thickness data in Figure 11 show that the fully developed film characteristics are nearly formed after ~10 h with an asymptotic approach indicated for the SWE thickness. In contrast, for the case of alkanethiolate SAMs on Au{111} both our own measurements and the literature show the full SAM characteristics almost are completely developed within minutes.[78,109,110] Note that the **ODT**/GaAs SAM assembly process can be broken into two

(106) Schreiber, F. *Prog. Surf. Sci.* **2000**, *65*, 151−256.

(107) Note that above 413 K precise the values of the peak frequencies show increasing error with increasing temperature since the corresponding intensities are becoming increasingly weaker.

(108) It has been noted that Ga−S bonds are more thermodynamically favored over As−S bonds and the latter begin to convert to Ga−S bonds at ~473 K. Scimeca, T.; Muramatsu, Y.; Oshima, M.; Oigawa, H.; Nannichi, Y. *Phys. Rev. B* **1991**, *44*, 12927−12932. If **ODT** monolayers bind predominately through As−S bonds, then the breaking of these bonds at ~473 K could be one explanation for the irreversible desorption of the **ODT** monolayers on GaAs.

(109) Jung, L. S.; Campbell, C. T. *Phys. Rev. Lett.* **2000**, *84*, 5164−5167.

(110) Jung, L. S.; Campbell, C. T. *J. Phys. Chem. B* **2000**, *104*, 11168−11178.

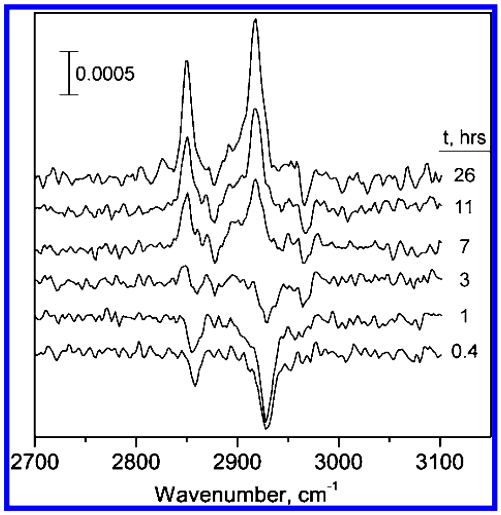

Figure 12. *p* polarized IRS spectra of the kinetic growth dependence of the **ODT** monolayers on GaAs (001). The IRS peaks are initially negative and slowly invert to the positive peaks observed for the full monolayers. See text for details.

distinct time regimes. The first includes a fast initial adsorption (regime I) in which the contact angles and SWE thickness rise to approximately 80% of their limiting values for a full monolayer.[111] This is followed by a much longer regime (II) in which incremental changes in thickness and contact angle are attributed to the spreading of lateral order throughout the monolayer. For the SAMs on Au, it has been reported that initial adsorption of nearly a full monolayer is complete within a few minutes, e.g., characterized by the achievement of an autophobic surface.[78,109,110] In contrast, for the **ODT**/GaAs SAMs, an autophobic surface was not observed until ~3 h, and only ~80% coverage was reached by ~12 h.

The IR data (Figure 12) show interesting trends in both peak frequencies and intensities. In the initial regime up to several hours, the d^+ and d^- modes exhibit peak positions of ~2855 and ~2929 cm^{-1}, respectively, with negative intensities. The shifts of +7 and +12 cm^{-1} compared to the well formed monolayers are a clear indication that the initially adsorbed chains are highly disordered. The negative intensities for an ideal all-*trans* chain would be associated with a tilt angle exceeding ~45°. Accordingly, the data suggest that each molecule on average has its overall molecular structure significantly more in contact with or closer to the surface than for a fully formed film. Note also the complete absence of the r_a^- mode and the very different intensity ratio of the d^+ and d^- peaks compared to the ratio of the full monolayer. These data all indicate a significantly different molecular structure compared to the full monolayer. Attempts to model these spectra in terms of actual molecular orientations were not done because of the high conformational disorder (see previous section).

In regime II between 3 and 7 h the CH_2 mode intensities flip sign, the peaks dramatically shift to lower frequencies (see Figure 11), and the r_a^- mode at 2967 cm^{-1} becomes observable. By ~7 h the organization of the chains appears to have "snapped" into place as judged by the sharp drop of the d^- mode's frequency to ~2917 cm^{-1}, a value associated with high conformational ordering. Longer times show continued, though small, decreases in frequency. Finally, the d^+/d^- ratio, which signals changes in average chain twist angles, slowly reaches the value of the fully formed SAM by 26 h. Overall, these data show that regime II involves primarily a final densification and lateral organization of the monolayer. A generalized picture of the assembly steps as deduced from the data is shown in Figure 13.

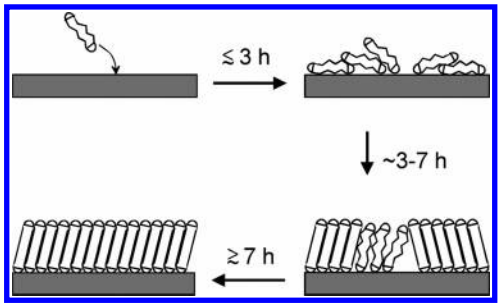

Figure 13. A generalized picture of the evolution of alkyl chain ordering during assembly of **ODT**/GaAs(001) SAMs. In the early stage the chains are conformationally disordered and exhibit a high degree of contact with the substrate. The second stage arises with a rapid onset of high conformational ordering, consistent with the formation of organized domains, and slowly proceeds with an asymptotic approach to a final highly organized assembly as the structure densifies.

While the two-step formation is mechanistically similar to alkanethiolate/Au{111} SAMs,[78,109,110] the much slower formation is striking. Since it has been observed for the SAMs on Au that surface contamination can significantly slow monolayer formation,[78] one could propose an analogous argument for GaAs involving, for example, the presence of some extent of an oxide phase which remains on the surface of the substrate after the etch step and slows SAM formation. Since the XPS data indicate no oxide in the final SAMs, any oxide on the etched initial substrate must have been removed during SAM formation. Another more intrinsic contribution to the slow rate could involve the activation barriers associated with the attachment chemistry of the thiol group to the bare GaAs substrate.

3.3.3. Exchange of SAM Molecules with Solute Thiols. As an initial test of the stability of the **ODT**/GaAs SAM toward exchange with solute thiol molecules, experiments were performed using deuterated **ODT** monolayers (*d*-**ODT**) as the host matrix. After recording an initial IR spectrum, each SAM was immersed in a 3 mM ethanolic solution of **ODT** for 24 h. The spectra in Figure 14 show a decrease in the intensity of C−D stretching modes along with the appearance of the C−H stretching modes. Comparison of the peak intensity of the initial C−D stretching mode to the same peak after exchange shows that ~30% exchange occurs. This exchange rate is similar to those for alkanethiolate/Au SAMs run under the same conditions.[112] At present the mechanism of the exchange process for the SAM on GaAs remains uncertain but it is clear that it is possible to be able to insert guest molecules into the host SAM matrix.

(111) We note that the contact angles approach approximately 80% of their limiting values within 1 h while IRS and SWE measurements do not show limiting values until ~7 h. This suggests, somewhat counterintuitively, that the surface regions of the samples are not fully disordered even at partial coverages. This behavior is not without precedent. Earlier work shows that even at ~50% coverage, alkyl chain structures prepared by grafting long chain alkanols with random placement on SiO_2 exhibit high HD contact angles, while IRS data show considerable disorder. These data were interpreted in terms of "tufting" of the alkyl chains near the surface. (Allara, D. L.; Parikh, A. N.; Judge, E. *J. Chem. Phys.* **1994**, *100*, 1761−1764).

(112) Smith, R. K.; McGuiness, C. L.; Uppili, S.; Weiss, P. S.; Allara, D. L., in preparation.

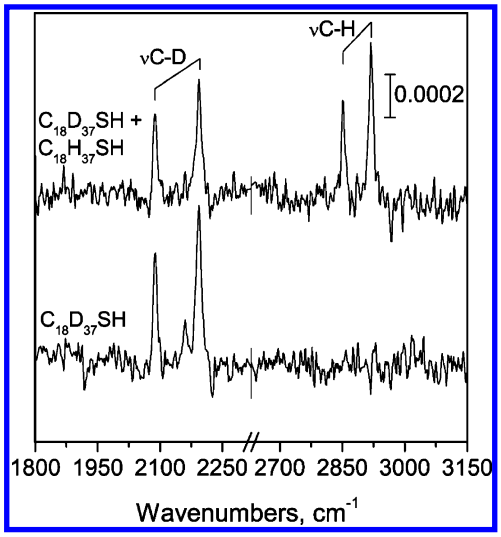

Figure 14. C−D and C−H stretching region IR reflection spectra of a fully deuterated **ODT**/GaAs(001) SAM monolayer (bottom) and after 24 h immersion in a 3 mM ethanol solution of protio **ODT** molecules (top). Integration of the peak areas and comparison with the pure deutero and pure protio SAM peak areas indicates ∼30% exchange with solute molecules.

4. Conclusions

This study shows that with careful control of substrate preparation and rigorous control of oxygen and humidity, **ODT** SAMs can be formed on GaAs(001) substrates in solution at room temperature with excellent reproducibility to yield highly organized, chemically stable structures with highly hydrophobic and oleophobic surfaces and direct substrate−molecule attachment. The high reproducibility allows definitive characterization of the intrinsic structure and indicates this structure represents a well-defined class of SAMs. The IRS and NEXAFS data lead to an average chain tilt of 14 ± 2° from the surface normal and an average chain twist of 43 ± 5°. The IRS data further show that the alkyl chains attain an average degree of conformational order similar to or exceeding the high order observed for **ODT**/Au{111} SAMs. The XPS data show that the SAMs strongly inhibit oxidation of the normally reactive GaAs(001) substrate for periods up to and even exceeding 2 weeks in ambient exposure. The absence of an oxide interface demonstrates direct molecule−GaAs attachment, but the current resolution of the XPS core level spectra does not allow determination of whether Ga−S, As−S, or some specific combination constitutes the interface bonding. High-resolution spectra are required to resolve the specific type of bonding, and preliminary results show evidence for As−S bonds.[113]

Although our data do not allow any direct interpretation of the adsorbate organization and correlation with the substrate structure, one can deduce some characteristics indirectly. In particular it is instructive to analyze the average chain tilts in terms of the average molecular spacings and compare these with the intrinsic GaAs(001) spacings (either As or Ga terminated). A simple geometric calculation for nearest neighbor (NN) chain tilting and an average chain diameter of ∼4.5 Å shows a 4.6 Å chain spacing for a 14° tilt (4.5/cos 14). In contrast, the NN spacing for the ideal (001) surface is 4.0 Å, much too small to accommodate adjacent chains. The next larger superlattice involves the next nearest neighbor spacing (NNN) [c(2×2) superlattice] at an ideal distance of 5.6 Å, much larger than the average 4.6 Å adsorbate spacing above for the 14° tilted chains; in contrast, tilts of ∼37° or higher would be required. Thus even with minor adjustments of tilt directions, it is clear that the adsorbates do not form a pattern that is even closely commensurate to an underlying ideal (001) lattice. Attempts to capture an image of the SAM using high resolution, contact mode AFM and He scattering were unsuccessful because of the easily damaged nature of the SAM and the inherent surface roughness (see Figure 1), respectively.[114] Recent attempts to use grazing incidence X-ray diffraction, however, do show evidence for translational ordering with a pseudo hexagonal structure aligned along the {220} crystal direction[115] and near vertically oriented chains.

With the above analysis in mind, one can reflect on our earlier report of the formation from molten thiol of an **ODT**/GaAs(001) SAM with chain tilt angles of ∼57°.[23] Given the relatively aggressive preparation conditions of many hours of heating at ∼100 °C in pure organothiol, it would not be unexpected to have significant reconstruction of the GaAs surface with the production of a different adsorbate structure than in the present case of room temperature solution conditions.[116]

In general, strong parallels exist between the **ODT**/GaAs(001) and **ODT**/Au{111} SAMs with respect to thermal behavior, formation characteristics, and susceptibility to exchange with solute organothiol molecules, though the specifics are different. First, it is clear that the **ODT**/GaAs(001) SAMs are thermally stable and resist desorption until elevated temperatures are reached. Our observations further show that these SAMs are less thermally stable than the corresponding Au{111} monolayers, though the comparison cannot be interpreted in a fundamental way at this time since the specific desorption mechanism is uncertain (e.g., Ga−S, As−S bond breaking or C−S bond breaking concerted processes involving C−H scission). Similar to the Au SAMs, with increasing temperature the chains first undergo limited conformational disordering then shift into desorption with continued disordering.

Second, the solution assembly of both the GaAs and Au SAMs follows a general type of two-step process with a rapid initial adsorption of molecules followed by a slow densification and self-organization process. The GaAs SAM, however, requires periods of hours for the initial process, in contrast to the periods of minutes for the Au SAM case. It is possible that this difference could be due to scavenging of traces of native oxides present on the GaAs surface and/or higher intrinsic

(113) McGuiness, C. L.; Shaporenko, S.; Zharnikov, M.; Walker, A. V.; Allara, D. L., in preparation.

(114) To directly image the tops of the molecules a minimum of 5 nN forces are typically used (e.g., for alkanethiolates/Au{111}). Use of these magnitude forces consistently resulted in damage to the samples, and reducing normal forces below the damage point did not result in molecular resolution. He scattering is well-known to be extremely sensitive to surface roughness and requires atomically smooth surfaces to produce diffraction peaks. In preliminary experiments only diffuse scattering of the He atoms was observed with no evidence for diffraction peaks. (Danisman, F.; McGuiness, C.; Scoles, G.; Allara, D., unpublished results).

(115) McGuiness, C. L.; Blasini, D. R.; Uppili, S.; Maciejewski, J. P.; Smilgies, D.; Allara, D. L., in preparation.

(116) Over an extended period working with this system, using many different preparation conditions, we have noticed that the alkanethiolate SAMs on GaAs(001) appear to fall into two classes of either a near vertical chain orientation or a highly tilted structure. This leads us to suspect that the GaAs surface is prone to reconstruction, especially at elevated temperatures, and that the process is somewhat driven by chain packing such that there are two preferred lattices with the lower temperature conditions leading to the spacings associated with near vertical chains.

kinetic barriers in establishing the thiol-GaAs bonding relative to the S−Au bonding.

Finally, in view of the large difference in the formation kinetics, it is interesting that solute exchange (insertion) rates of the SAMs on GaAs and Au appear to be quite similar overall. This result suggests that the exchange mechanisms could be quite similar. No information, however, is presently available on the detailed kinetic rate laws so further studies would be necessary to reveal any mechanistic differences. The ability of the SAMs on GaAs(001) to undergo exchange opens up the possibility of insertion of a variety of organothiol molecules with interesting functionality, e.g., electrical (molecular wires and switches) and photoactive molecules, and such studies are underway in our labs.

Acknowledgment. The authors gratefully acknowledge financial support from The Defense Advanced Project Agency (D.A., S.U. and C.M.), the National Science Foundation (Pennsylvania State University MRSEC Grant No. DMR-0080019, C.M.), and the German BMBF (05KS4VHA/4; A.S. and M.Z.). The authors also acknowledge the experimental assistance of Gordon Tseng and Erwin Vogler with the Wilhelmy balance measurements, M. Grunze and Ch. Wöll for providing experimental equipment in the NEXAFS experiments, and the assistance of the BESSY II staff during the synchrotron runs.

Supporting Information Available: NEXAFS angular dependencies for **ODT**/GaAs and **HDT**/Au; IRS signal dependence with angle of incidence; Response of individual IR modes with beam polarization; XPS spectra showing oxide growth with time; IRS spectra of **ODT**/Au and **ODT**/GaAs SAMs before and after heating. This material is available free of charge via the Internet at http://pubs.acs.org.

JA058657D